



## Original article

Neuroprotective effects of phenylacetylglycine via  $\beta$ 2AR on cerebral ischemia/reperfusion injury in ratsWenjie Hu<sup>a</sup>, Xueyan Kuang<sup>b</sup>, Yao Zhang<sup>a</sup>, Yimin Luo<sup>a</sup>, Litao Zhang<sup>a,\*</sup><sup>a</sup> School of Biological Science, Jining Medical University, Rizhao 276826, Shandong Province, PR China<sup>b</sup> Qingdao West Coast New Area Center for Disease Control and Prevention, Qingdao 266427, Shandong Province, PR China

## ARTICLE INFO

## Keywords:

Phenylacetylglycine (PAGly)  
Ischemia/Reperfusion Injury (I/R injury)  
Microglia  
 $\beta$ 2-adrenergic Receptors ( $\beta$ 2AR)  
Neuroprotective

## ABSTRACT

Phenylacetylglycine (PAGly) is a small molecule derived from phenylalanine in the gut via glycine degradation and conjugation. It has been associated with both the progression of atherosclerosis and protective effects on the myocardium. This study evaluated the function and the underlying mechanisms of PAGly in a rat cerebral ischemia/reperfusion (I/R) injury model. The results indicated that PAGly markedly alleviated cerebral infarct volume ( $P = 0.0024$ ) and improved the neurobehavioral outcomes ( $P = 0.0149$ ) after I/R injury. PAGly is structurally analogous to catecholamines and binds to  $\beta$ 2-adrenergic receptors ( $\beta$ 2AR) on microglia without altering the expression of these receptors ( $P = 0.9137$ ), but instead inhibiting their activity. It was also observed that when  $\beta$ 2AR was engaged in microglia, PAGly suppressed the release of TNF- $\alpha$  ( $P = 0.0018$ ), IL-1 $\beta$  ( $P = 0.0310$ ), and IL-6 ( $P = 0.0017$ ), thereby reducing neuronal apoptosis ( $P = 0.000003$ ). Furthermore, the protective effect of PAGly diminished after the administration of  $\beta$ 2AR-specific agonist fenoterol ( $P = 0.0055$ ). These data indicate that PAGly mitigates cerebral I/R injury by inhibiting microglial inflammation via  $\beta$ 2AR, highlighting its potential as a therapeutic agent. These findings position PAGly as a promising candidate for therapeutic intervention in cerebrovascular injuries, warranting further exploration in clinical settings.

## 1. Introduction

Stroke is a leading cause of mortality worldwide and is primarily caused by cerebral ischemia (Fan et al., 2023). Cerebral ischemia/reperfusion (I/R) injury is characterized by temporary obstruction in the cerebral circulation and can cause irreversible neurological damage. Furthermore, it can also result in thrombosis, embolism, or reduced blood flow, which can potentially result in fatal outcomes or persistent impairment (Prabhakaran et al., 2015). Currently, the most commonly employed therapeutic agent for ischemic stroke is recombinant human tissue-type plasminogen activator (rt-PA), which can stimulate revascularization in a short period and thus achieve therapeutic goals. However, rt-PA has an extremely narrow therapeutic window, and most patients lose the optimal treatment time (Hacke et al., 2004). Alterations in energy metabolism, the induction of oxidative stress and inflammatory responses, as well as the activation of apoptotic pathways are critical for the development of cerebral I/R injury following ischemic strokes (Jin et al., 2013). Moreover, neuroinflammation and oxidative stress are the primary mechanisms driving neuronal injury and programmed cell death during these events (Wang et al., 2024; Wu et al.,

2020). Therefore, rt-PA therapy, as well as the suppression of post-stroke neuroinflammation, are important research directions for the treatment of cerebral I/R injury.

With the burgeoning interest in the brain-gut axis research, the role of intestinal microbiota and their metabolites in modulating neuroinflammation subsequent to cerebral I/R injury has garnered significant attention and appreciation (Benakis et al., 2016; Hu et al., 2022). Intestinal microbiota can convert phenylalanine in the diet into phenylacetic acid, which, in conjunction with glycine, synthesizes phenylacetylglycine (PAGly) (Romano et al., 2023). The literature has indicated that PAGly is a bioactive metabolite that can enhance the adhesion of platelets with collagen, increase  $\text{Ca}^{2+}$  elevation in response to platelet stimuli, and promote dose-dependent platelet aggregation (Nemet et al., 2020). However, it has also been suggested that PAGly promotes protective effects during myocardial I/R injury as its administration has been observed to reduce apoptosis and infarct size, although high doses are linked with increased mortality (Xu et al., 2021). Furthermore, during acute liver failure, PAGly production is an effective pathway for ammonia detoxification (Kristiansen et al., 2014). Moreover, supplementing probiotics to animals can influence the serum

\* Corresponding author at: School of Biological Science, Jining Medical University, Rizhao 276826, Shandong Province, PR China.

E-mail address: [zhanglitao@mail.jnmc.edu.cn](mailto:zhanglitao@mail.jnmc.edu.cn) (L. Zhang).<https://doi.org/10.1016/j.jsps.2024.102210>

Received 4 July 2024; Accepted 25 November 2024

Available online 26 November 2024

1319-0164/© 2024 The Author(s). Published by Elsevier B.V. on behalf of King Saud University. This is an open access article under the CC BY-NC-ND license (<http://creativecommons.org/licenses/by-nc-nd/4.0/>).

concentration of PAGly by altering the gut microbiota, indicating its relevance in gut health and broader metabolic functions (Adeyemi et al., 2020).

Overall, the research on PAGly remains in its early stages. Although the research on the gut-brain axis has advanced rapidly in recent years,

the specific role of PAGly in the nervous system remains unknown. Therefore, this investigation aimed to elucidate the impact of PAGly on the central nervous system, its neuroprotective or neuroactive roles in brain injury, and the related underlying processes using a rat cerebral I/R model.

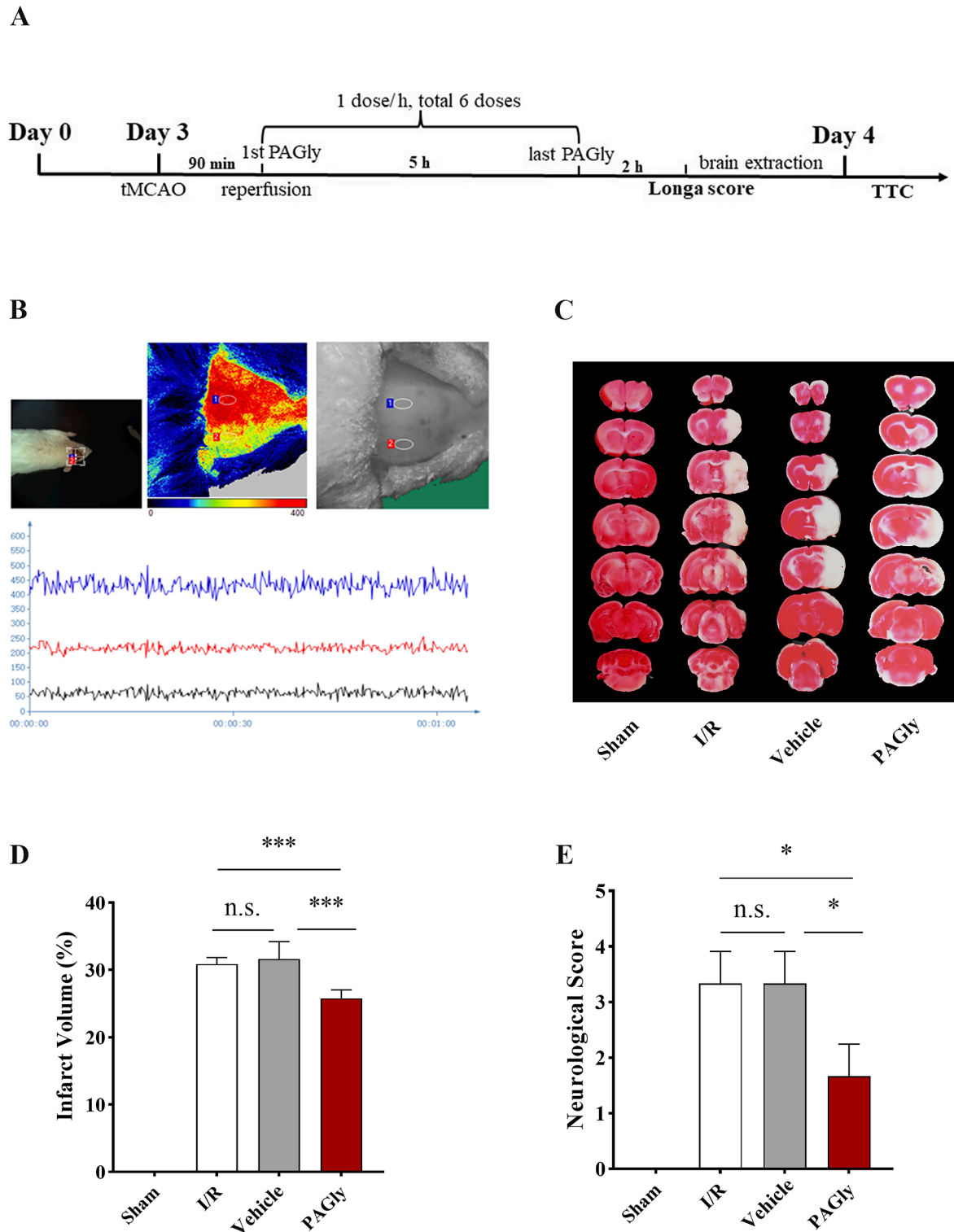


**Fig. 1.** PAGly attenuates cerebral injury after I/R. A. Flow chart of animal experiment. B. Dynamic flowmetry results after suture insertion. Region 1 represents the healthy side, while region 2 depicts the site of suture insertion, which is indicated by the yellow coloration due to the reduction in blood flow. C. TTC staining results of brain tissues obtained from the four groups with different treatments, the white areas are defined as infarcted areas. D. Statistical analysis of infarcted area. E. Neurological impairment function scores of rats in the four groups after treatment respectively (For all panels, \* $P < 0.05$ , \*\*\* $P < 0.01$ , n.s., no significance,  $n = 3$ ). Results are represented as means  $\pm$  S.D. by ANOVA.

## 2. Methods and materials

### 2.1. Animals & groups

The weight range of 200–220 g for male Sprague-Dawley rats ensures suture compatibility in middle cerebral artery occlusion (MCAO) models, aiding in the avoidance of estrogen's potential confounding effects (Merchenthaler et al., 2003). Rats were sourced from Jinan Pengyue (SCXK-Lu-2022–0006), acclimatized for 7 days prior to experimentation. Animal handling was carried out following the Guide for the Care and Use of Laboratory Animals (National Institutes of Health publication 86–23, 1985 revision). The rats were housed in cages (n = 2–3 animals/cage) under a 12-hour light/dark cycle at a constant temperature of 23–25 °C and 35 ± 5 % humidity. All the rats were randomly categorized into 4 groups: Sham, I/R, Vehicle (I/R + PBS treatment), and PAGly (I/R + PAGly treatment) groups. All experiments were conducted by investigators who were blinded to the group assignments. Fig. 1A indicates the detailed protocol of the animal experiments. All the animal protocols were authorized by the Animal Care Committee of Jining Medical University (Approval No. JNMC-2023-DW-085) and followed the Guide for the Care and Use of Laboratory Animals.

### 2.2. tMCAO/reperfusion (I/R)

The suture occlusion technique was employed to operate the transient MCAO (tMCAO), as described in our previous study (Xu et al., 2021). The rats were anesthetized with a Small animal anesthesia system (R550, RWD, China). Briefly, the rats were placed in the anesthesia induction box, which was turned on to let isoflurane in the environment. The isoflurane gas induction volume was 4–5 % with an oxygen flow rate of 1–2 L/min for several mins. The depth of anesthesia was assessed by pinching the rat's tail and observing the presence or absence of nerve reflexes. For the maintenance phase, the isoflurane concentration was reduced to 1–1.5 %, with an oxygen flow rate of 0.5–1 L/min (Gargiulo et al., 2012). The heart rate of the rats was maintained between 250–450 bpm. Body temperature was maintained during and after surgery. During the surgery, the common carotid artery (CCA) was exposed by making a mid-cervical incision. Then, after careful separation, an L3200 wire suture (Jialing, China) was inserted (approximately 22 mm) into the internal carotid artery (ICA) via the external carotid artery (ECA). Reperfusion was initiated by removing the suture after 90 min of occlusion, then the ECA was secured, and the surgical site was sutured closed. Sham-operated rats also received a similar surgical protocol, excluding the suture insertion and subsequent removal. Animals with failed model induction or incomplete brain extraction were excluded from the analysis. All animals were housed individually after surgery, with the incision site disinfected and body temperature maintained using heating pads. Soft food was provided, and the animals were continuously monitored.

### 2.3. Drug administration

PAGly (MFCD00021744, MACKLIN) dose of 20 mg/kg was selected for *in vivo* experiments based on a previous study (Xu et al., 2021). Preliminary results showed that this dose was safe for animals. Briefly, PAGly was dissolved in PBS and then intraperitoneally injected into the rats immediately after pulling out the suture. The second dose was given 1 h later at half the original amount. Then, the dose was halved every 1 h for a total of 6 injections. The vehicle group received the same treatment, but instead of PAGly, they were injected with PBS. Sham and I/R groups were left untreated after the surgery was completed.

### 2.4. Assessment of neurological scores

The neurological assessments were conducted 24 h post-reperfusion, succeeding a 90-min ischemic period, and followed the methodology

outlined by Longa et al. (Longa et al., 1989).

### 2.5. Brain extraction and TTC staining

Drug administration was completed 5 h after suture removal, and the rats were euthanized after 2 h of the drug administration. The rat skulls were carefully dissected to obtain intact brains. For euthanasia, the animals were overdosed with pentobarbital sodium (P3761, Sigma) injection, decapitated, and their brain tissues were collected. For TTC staining, the brains of most rats were harvested 24 h after reperfusion. Post-decapitation, brains were sectioned (2 mm), incubated in 2 % TTC (R20618, Yuanye) at 37 °C for 30 mins, then preserved at 4 °C in 4 % paraformaldehyde for 24 h (Chen et al., 2022). Image handling and analysis were blinded, under controlled lighting, using Image-Pro Plus 6.0 software.

### 2.6. Western blot analysis

The extracted ischemic penumbra proteins were subjected to the BCA method, 10 % SDS-PAGE separation, transferred to the membrane, occluded in 5 % BSA for 2 h, and treated with primary antibody against AKT (1:1000, ab8805, Abcam), pAKT (1:1000, ab66138, Abcam) PTEN (1:1000, 9559, CST),  $\beta$ 2AR (1:1000, AG1054, Beyotime), and  $\beta$ -actin (1:4000, K200058M, Solaibio) at room temperature 20 min and then at 4 °C overnight. The membranes were then probed with HRP goat anti-rabbit or rat IgG (1:1000, SE134, SE132, Solarbio) antibody, and the blots were detected using the Invitrogen iBright CL1500 imaging system.

### 2.7. Molecular docking

The PAGly's SDF file and  $\beta$ 2-adrenergic receptors ( $\beta$ 2AR) structure were acquired from the PubChem and PDB databases, respectively. The Pymol software was employed to optimize the target by removing small-molecule ligands and water molecules. Furthermore, the AutoDock Tools were utilized for charge processing and hydrogenation, which were saved in the pdbqt format. Molecular docking was performed via the Vina package of the Pyrx software, using the key target as the receptor and its corresponding active ingredient as the ligand to evaluate the binding energy and result file output. The PyMol software was employed to visualize the results. The affinity value (kcal/mol) indicated the binding ability of the two ligands and the receptor, where the lower binding capacity represented a more stable ligand-receptor binding. For the 3D visualization and 2D plots analysis, PyMol and Discovery Studio 2020 Client were employed, respectively.

### 2.8. Cell culture and RT-qPCR

BV2 cells were procured from Wuhan Pricella Biotechnology Co., Ltd. and cultured per the manufacturer's guide. Total cellular RNA was isolated using the RNAfast 200 purification kit (220011, Fastagen), reverse transcribed with HiScript IV RT SuperMix for qPCR (+gDNA wiper) (R423-01, Vazyme), and subjected to RT-qPCR analysis using the FastSYBR Mixture (CW0955M, CWbio) on a Bio-rad CFX96 instrument.

**Table 1**  
Primer Sequences.

Primer	Sequence
IL-1 $\beta$	5'-CTATGGCAACTTCCCTGAA-3' 5'-GGCTTGGAAAGCAATCCTTAATC-3'
TNF- $\alpha$	5'-TTCTGTCTACTGAACTTCGGGGTGATGGGTCC-3' 5'-GTATGAGATAGCAAATCGGCTGACGGTGTGGG-3'
IL-6	5'-GACTGATGTTGTTGACAGCCACTGC-3' 5'-TAGCCACTCCTTCTGTGACTCTAACT-3'
GAPDH	5'-TGGTGAAGGTCGGGTGGAACGG-3' 5'-ACTGTGCCCTTGAATTTGCCG-3'

Table 1 enlists the sequences of primers utilized for RT-qPCR.

### 2.9. Enzyme-linked immunosorbent assay (ELISA)

ELISA was carried out per the guidance of the kits (MM-0390R1, MM-0160R1, MM-0807R1, Meimian, China). Briefly, the supernatant of the BV2 culture was aspirated and centrifuged for 10 mins at 3000 rpm. Then, the samples and the standards were added to the plate wells and treated with HRP-labeled antibodies for 60-mins at 37 °C, washed, and then incubated with substrate solution at 37 °C for 15 mins in the dark. After the reaction termination, the optical density (OD) values were measured at 450 nm, and a standard curve was drawn to assess the concentrations (Lin et al., 2021).

### 2.10. Conditioned medium assays

The neuroprotective effect of PAGly was investigated using the conditioned medium system. Briefly, the BV2 cells were inoculated and pretreated with PAGly or PBS (50 µM) for 24 h and then stimulated for 8 h with LPS (0.1 µg/mL, L2880, Sigma). The fenoterol (1 µM, HY-B0976, MCE) was added based on the animal grouping (Wang et al., 2016). Following treatment, each group was co-cultured with primary neurons using respective conditioned media.

### 2.11. Primary neuron culture

Primary rat neurons were isolated from embryonic rat brains. After the dissection process, samples were subjected to enzymatic dissociation using 0.25 % trypsin for 15 min at 37 °C, followed by mechanical trituration to further dissociate the cells. The acquired cell suspension was then filtered and centrifuged for cell purification. The neurons were resuspended in a neurobasal medium enriched with L-glutamine, B27 supplement, and antibiotics. The resultant suspension was then cultured in poly-D-lysine pre-coated plates (which enhanced cell adhesion) at 37 °C and 5 % CO<sub>2</sub>. For optimal growth conditions, half of the medium was replaced every 3–4 days to provide fresh nutrients and remove cellular debris (Wang et al., 2024).

### 2.12. Cell immunofluorescence

This experiment was carried out by following a previously described protocol (Onasanwo et al., 2016). Briefly, the cells were preserved with 4 % PFA for 10 min, permeabilized with 0.5 % Triton X-100 for 10 min, blocked for 2 h in 5 % BSA-PBS, treated overnight with primary antibodies at 4 °C, and then probed with secondary antibodies at room temperature for 1 h. The cells were then stained with DAPI for 5-min, coverslipped, and then observed and imaged via a confocal microscope (Leica STELLARIS5, Germany).

### 2.13. Detection of neuronal apoptosis by flow cytometry

The Annexin V-FITC Apoptosis Detection Kit (556547, BD) was employed to assess the apoptosis rate. Briefly, the cells were pre-treated with the conditioned medium, digested for 3 mins with 0.25 % trypsin, neutralized with 10 % FBS medium, gently pipetted, and centrifuged. Then, the cells were adjusted to 10<sup>6</sup>/mL concentration, washed with PBS, resuspended in 1 × binding buffer, dyed with PI and Annexin, and diluted in the banding buffer (500 µL) before analysis with flow cytometry (BECKMAN COULTER, CA, USA). Finally, the percentage of PI positives was assessed (Wu et al., 2022).

### 2.14. Statistical analysis

For all the statistical measurements, GraphPad Prism 9.0 software was employed, and the measured values are indicated as means ± SD. Multigroup comparisons was carried out using ANOVA with post hoc

contrasts by Tukey's tests, comparisons between two groups were made using the Student-*t* test. Group assignments were blinded to the statisticians involved in the data analysis. Differences were deemed statistically significant at  $P < 0.05$ .

## 3. Results

### 3.1. PAGly significantly diminished infarct size and improved neurological function

The dynamic monitoring of the cerebral blood flow indicated that the blood flow at the suture-inserted side was maintained at the baseline level of 210 perfusion unit (PU), and the site was yellow, whereas the healthy side was red with the blood flow was about 450 PU, which indicated that the blood flow decreased significantly, and the modeling was successful (Fig. 1B). To visualize the changes in the ischemic region after PAGly application, TTC staining was performed on the brains of different rat groups. The results indicated a lack of infarct area in the Sham group. Whereas white infarct areas were observed in the I/R, Vehicle, and PAGly groups (Fig. 1C). Furthermore, compared with the I/R group, no significant changes were observed in the percentage of infarct volume after PBS application ( $P = 0.8953$ ); however, there was a significant decrease in the percentage of infarct volume after the PAGly treatment ( $P = 0.0024$ , Fig. 1D). Moreover, compared with the I/R group, the Longa score results showed no significant difference in neurological deficits in the Vehicle group ( $P = 0.8452$ ) but had reduced neurological impairment in the PAGly group ( $P = 0.0149$ , Fig. 1E). This indicates that PAGly can reduce the infarct volume in cerebral I/R and enhance neurological behavioral functions, thereby exerting a protective effect on injury brain.

### 3.2. PAGly increases cell survival without altering β2AR expression

To further evaluate how PAGly promotes these protective effects, Western blot analyses were conducted on the brain tissue samples from the ischemic penumbra. These samples were collected because, during the I/R process, salvageable neurons are predominantly located within the penumbra. Therefore, the penumbra represents a critical area for implementing neuroprotective strategies (Ermine et al., 2021). The pAKT to AKT ratio is commonly employed to indicate cellular survival (Yang et al., 2016). The Western blot was carried out to determine the contents of AKT and pAKT in the ischemic penumbra (Fig. 2A). Compared with the Sham group, pAKT/AKT was notably reduced in the I/R group ( $P = 0.00005$ ). Furthermore, there was no significant change in the Vehicle group relative to the I/R group ( $P = 0.9914$ ); however, the I/R + PAGly group had an increased ratio compared with the I/R group ( $P = 0.0008$ , Fig. 2B). The previous literature has demonstrated that the inhibition of PTEN during I/R promotes neuroprotection (Liu et al., 2010; Zhang et al., 2020). Therefore, the PTEN expression was also assessed in this study, which revealed markedly increased PTEN expression in the I/R group compared with the Sham group ( $P = 0.0001$ ). Whereas there was no significant difference in the PTEN expression between the I/R and PBS-treat groups ( $P = 0.3233$ ). In contrast, the PTEN expression was reduced in the PAGly-treat group compared with the I/R group ( $P = 0.0017$ , Fig. 2C). This outcome is consistent with the results of prior studies.

Since PAGly has been observed to act through β2AR (Xu et al., 2021), this investigation also evaluated the expression of β2AR. The data indicated that the expressions did not change among the four groups ( $P = 0.9984$ ,  $P = 0.7015$ ,  $P = 0.9137$ , respectively. Fig. 2D, E), suggesting that PAGly does not alter the protein levels of β2AR. The comparison of the molecular structure of PAGly with other adrenergic hormones revealed significant similarities (Fig. 2F). In addition, the molecular docking of PAGly with β2AR using the Discovery Studio 2020 software indicated that PAGly has a strong binding capacity with β2AR, with the affinity value of  $-6.7$  kcal/mol. (Fig. 2G).



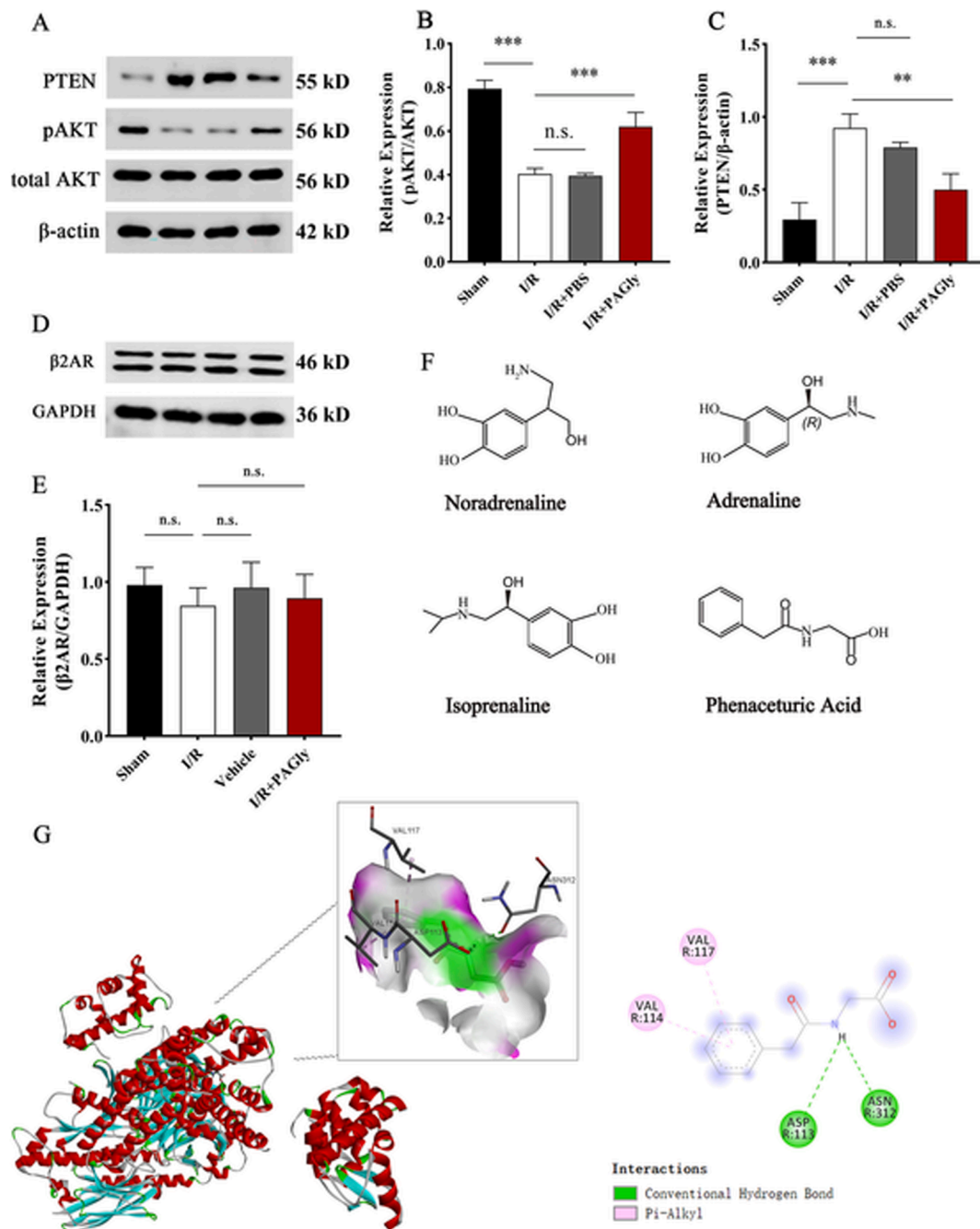


**Fig. 2. PAGly does not alter β2AR expression but increases penumbra cell viability.** A. Western blot showing PTEN, pAKT and AKT expressed in different groups. B. The statistics of the ratio of pAKT to total AKT showed that the expression of pAKT was reduced by the I/R treatment ( $***P < 0.01$  vs sham,  $n = 3$ ), PBS had no significant effect (n.s., no significance vs I/R,  $n = 3$ ), and the PAGly treatment reversed the reduction of the expression caused by the I/R ( $***P < 0.01$  vs sham,  $n = 3$ ). All results are represented as means  $\pm$  S.D. by ANOVA. C. PTEN expression was significantly increased following I/R ( $***P < 0.01$  vs sham,  $n = 3$ ); PBS injection had no effect on PTEN expression following I/R (n.s., no significance vs I/R,  $n = 3$ ), which was significantly reduced following PAGly injection ( $**P < 0.05$  vs I/R,  $n = 3$ ). D. The statistics of the β2AR expression showed that no significant difference was observed in the comparison among the four groups (n.s., no significance,  $n = 3$ ). D. Western blot result of β2AR under different treatment. E. The expression of β2AR was not altered following different treatments. F. Chemical structure of norepinephrine, adrenaline, isoprenaline and PAGly. G. Results of the protein-small molecule docking of the β2AR with PAGly. The protein structure shown in the Fig. is β2AR, and the small molecule shown in gray is PAGly.

### 3.3. PAGly regulates microglia polarization through β2AR

Since β2AR can bind PAGly, how PAGly exerts its effects within brain tissue following administration was assessed. Microglia in brain tissue express β2AR (Sugama et al., 2019; Damo et al., 2023). During the early stages of I/R injury, activated microglia secrete various inflammatory factors, including IL-1β, IL-6, and TNF-α, which exacerbates the local pathological processes (Liu et al., 2020). Therefore, the present study

investigated whether PAGly exerted a protective effect by modulating the microglial inflammatory processes. After 24 h of PAGly pretreatment, the expression of TNF-α, IL-1β, and IL-6 mRNA in microglia showed varying degrees of reduction upon subsequent LPS stimulation ( $P = 0.0016$ ,  $P = 0.0009$ ,  $P = 0.0409$ , respectively. Fig. 3A, B, C). iNOS is recognized as a marker of the inflammatory state of microglia (Zhou et al., 2021). Here, the immunofluorescence staining revealed markedly increased iNOS expression in BV2 cells after LPS stimulation ( $P =$

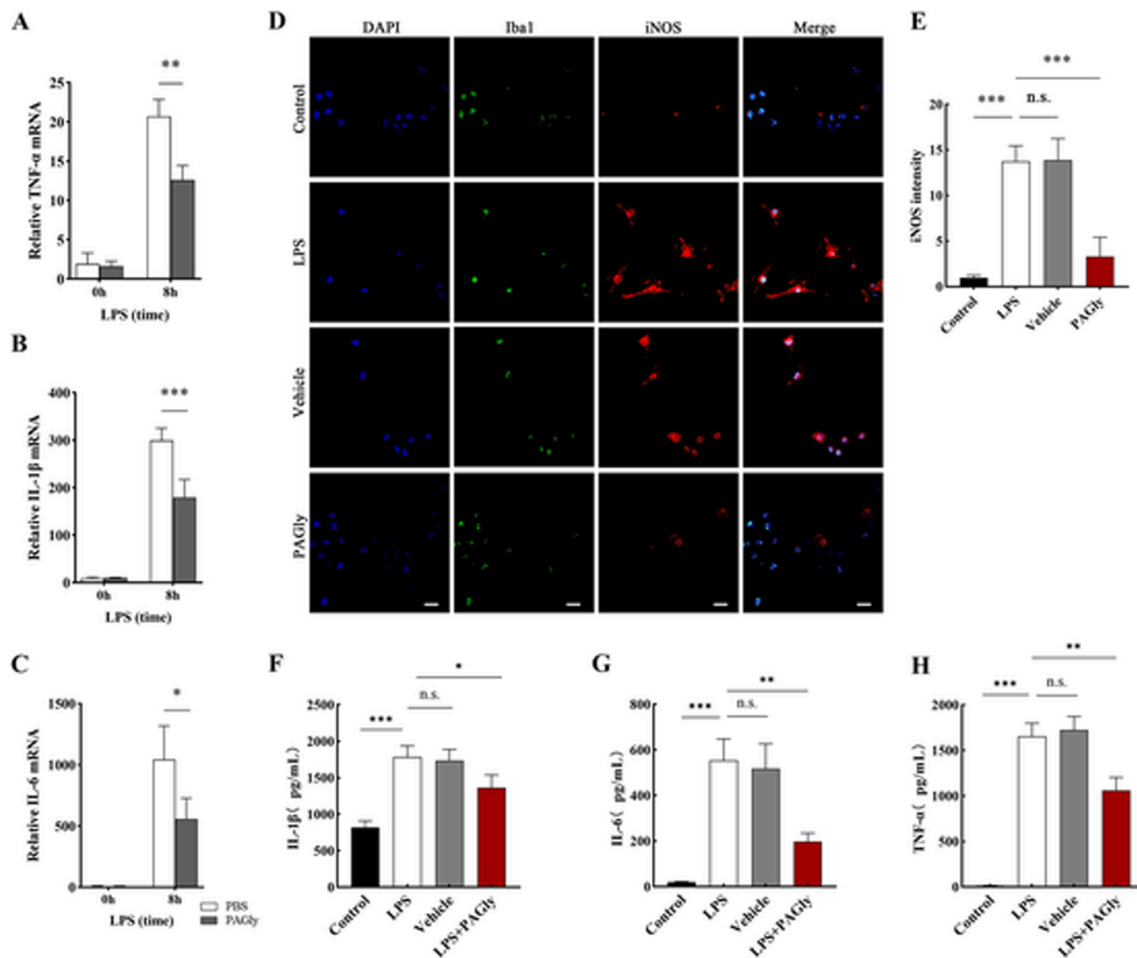


**Fig. 3.** PAGly alleviates microglial inflammatory response after LPS stimulation. A-C. RT-qPCR analysis of TNF- $\alpha$ , IL-1 $\beta$ , and IL-6 ( $n = 3$  from three independent experiments) mRNA expression in BV2 microglia pretreated with PBS or PAGly followed by treatment with LPS for 8 h. D. Representative image showing immunofluorescence staining of iNOS, Iba-1, and DAPI in BV2 microglial cells intervened with PBS or PAGly and treated with PBS or LPS for 4 h. Scale bars, 10  $\mu\text{m}$  ( $n = 6$  from 6 individual biological samples). LPS stimulation significantly increased microglial cell size and iNOS expression, and the addition of PBS did not alter their inflammatory characteristics. iNOS expression decreased and cell size was smaller after PAGly intervention. E. Immunofluorescence statistical results of iNOS. F-H. ELISA results for the detection of IL-1 $\beta$  (F), IL-6 (G) and TNF- $\alpha$  (H) in BV2 supernatants after different treatments.

0.0001), which was reduced after pretreatment with PAGly ( $P = 0.0004$ ). Moreover, LPS stimulation induced enlargement and rounding of BV2 cell bodies, indicating morphological polarization, which can be reversed by PAGly treatment (Fig. 3D, E). ELISA analysis of inflammatory factors in BV2 supernatants following various treatments demonstrated that the levels of IL-1 $\beta$ , IL-6, and TNF- $\alpha$  exhibited varying degrees of attenuation following pretreatment with PAGly ( $P = 0.0310$ ,  $P = 0.0017$ ,  $P = 0.0018$ , respectively. Fig. 3F, G, H). These data are consistent with the hypothesis, suggesting that PAGly promotes a neuroprotective effect following I/R, which might be mediated by inhibiting microglial polarization.

### 3.4. PAGly protects neurons by reducing the inflammatory response via $\beta$ 2AR

To validate that PAGly works in conjugation with  $\beta$ 2AR, thereby inhibiting its activity, the effect of fenoterol, a  $\beta$ 2AR-specific agonist, was investigated (Wang et al., 2022) to examine whether the former anti-inflammatory effect was diminished. Briefly, primary neurons were co-cultured for 12 h with the conditioned medium of BV2 treated differently. The immunofluorescence staining of these cells revealed that the control group neurons had regular morphology with long and well-defined axons, while the neurons in the PBS group had impaired morphology and shorter axons. Furthermore, the PAGly group neurons

had partially restored morphology and distinct axons; however, the number of cells was lower relative to the control group. Moreover, the concomitant use of PAGly and fenoterol reduced the initially observed protective effect and decreased the cell survival (Fig. 4A). This implies that PAGly mitigates the inflammatory response in BV2 cells via  $\beta$ 2AR and, thus, confers a neuroprotective effect. However, this protective mechanism is counteracted by the specific agonist fenoterol.

This study also carried out flow cytometry to elucidate the apoptosis rate of neurons following different treatments. The data revealed that the LPS-treated microglial medium markedly increased the apoptotic rate, characterized by the increased number of cells in the Q2 region ( $P = 0.000072$ ). However, this damaging effect was mitigated by PAGly treatment, which decreased the number of apoptotic cells ( $P = 0.000003$ ), but the addition of fenoterol neutralized this protective effect ( $P = 0.0055$ ) (Fig. 4B, C).

## 4. Discussion

Phenylalanine in food undergoes microbial action to transform into phenylacetate, which then combines with glycine to synthesize phenylacetylglutamine, also known as PAGly. PAGly has a molecular weight of  $< 200$ , which allows it to cross the blood-brain barrier (BBB) and perform direct action (Nair et al., 2018). Here, it was observed that PAGly administration reduced the infarct size and improved the

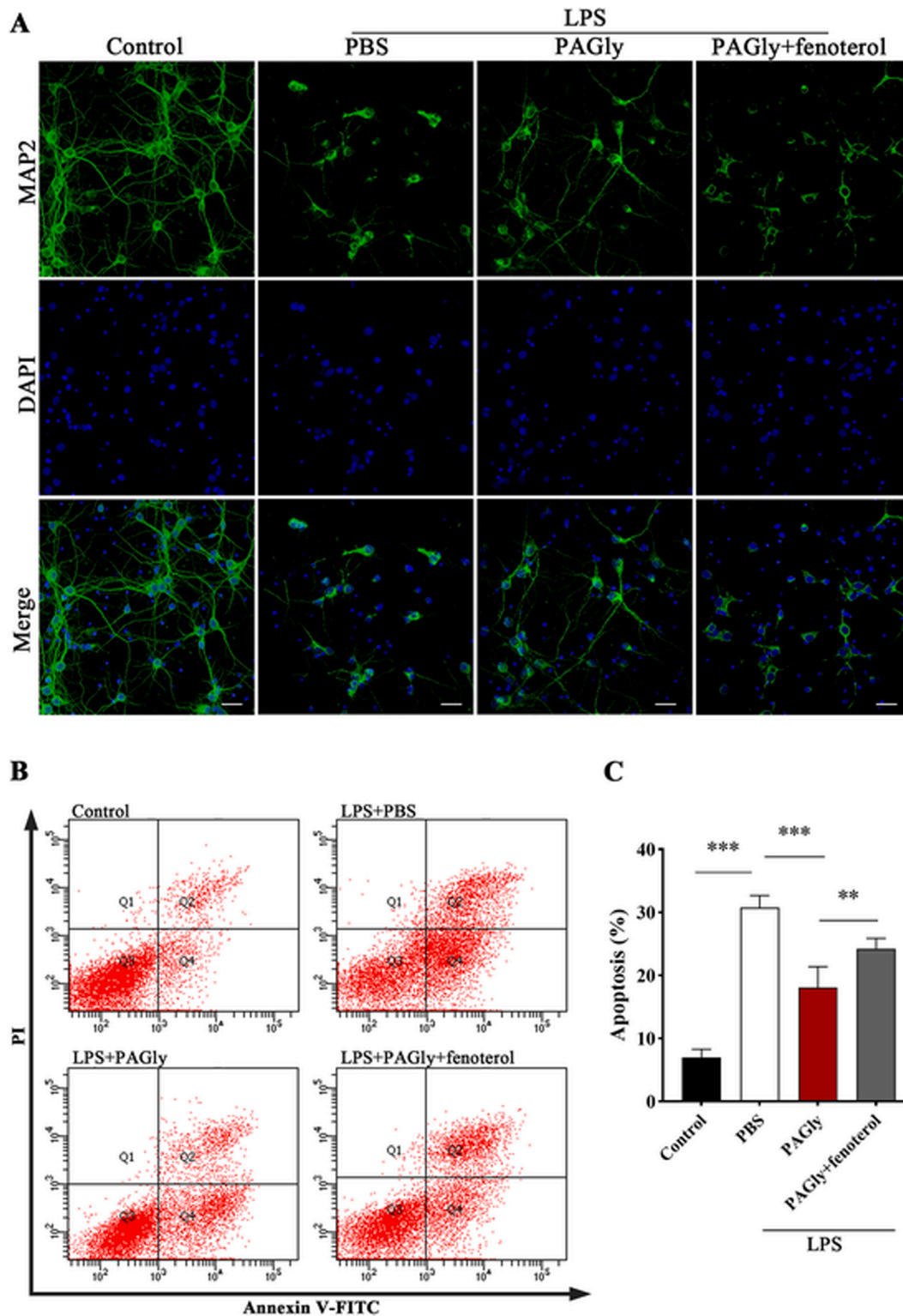


**Fig. 4.** PAGly reduces apoptosis of primary neurons by suppressing microglial inflammation via  $\beta$ 2AR. **A.** Representative immunofluorescence staining of MAP2 in primary cortical neurons. Scale bars, 100  $\mu$ m ( $n = 6$  from six individual biological samples). After LPS treatment of BV2, the conditioned medium reduced the number of neurons, shortened axons, and caused irregular morphology. The morphologic damage was ameliorated by PAGly intervention. The neuroprotective effect of PAGly was reversed by the addition of the  $\beta$ 2AR-specific agonist fenoterol. **B.** Flow assay for neuronal apoptosis after co-culture in conditioned media with different treatment. **C.** Statistical results of early apoptosis rate of neurons after different treatments in four groups.

neurological behavioral scores in I/R rats. Since PAGly has been observed to exert protective effects in myocardial ischemia through  $\beta$ 2AR (Xu et al., 2021), it was evaluated whether PAGly acts through  $\beta$ 2AR during cerebral I/R processes. The data revealed that the  $\beta$ 2AR

expression did not change before and after the administration of PAGly. This raises the question of whether PAGly is unable to bind to  $\beta$ 2AR. Comparative structural analysis revealed similarities between the molecular structure of PAGly and  $\beta$ 2AR hormones. Furthermore, molecular

docking indicated that PAGly could bind  $\beta$ 2AR. Moreover, PAGly diminished the secretion of inflammatory cytokines in LPS-induced BV2 cells, thereby reducing neuronal apoptosis; however, this effect was attenuated by the addition of a  $\beta$ 2AR agonist.

Several studies have highlighted that association of neuroinflammation mediated by activated microglia with the pathogenesis of ischemic stroke (Wang et al., 2020; Peng et al., 2022). Upon activation, microglia can be polarized into two phenotypes, M1 and M2 (Jin et al., 2023). During acute stress, microglia within various brain regions, such as the hippocampus, thalamus, and cerebellum, are activated and enhance the expression of  $\beta$ 1AR and  $\beta$ 2AR. This microglial activation results in an increased number of microglia, which are characterized by enlarged cell bodies and enhanced IL-1 $\beta$  secretion (Tanaka et al., 2002; Sugama et al., 2019); this phenomenon represents the M1 type of transformation. The literature has revealed that PAGly exerts its effects via the  $\beta$ 2AR (Xu et al., 2021). Therefore, the present study also investigated whether the observed brain-protective effects were mediated by the  $\beta$ 2AR in microglia. However, the acquired data indicated that  $\beta$ 2AR expression levels after I/R were independent of PAGly used. Since the molecular docking indicated that PAGly has a strong binding affinity with  $\beta$ 2AR, it was inferred that PAGly can inhibit microglial inflammation. Following LPS stimulation, inflammatory factors secreted by BV2 exhibited differential elevation, indicative of microglial M1-type transformation. Furthermore, after PAGly therapy, the levels of inflammatory cytokines, as well as iNOS expression in microglia, were reduced markedly. These observations collectively indicated the occurrence of M2-type transitions.

Numerous studies have demonstrated that early inhibition of microglial M1 polarization in cerebral I/R injury can reduce the secretion of inflammatory mediators, promote M1 to M2 transition, decrease infarct volume, and confer neuroprotection (Liao et al., 2020; Zhu et al., 2021; Liang et al., 2023; Xu et al., 2023). Moreover,  $\beta$ -blockers have been observed to markedly reduce brain infarct size in rat's cerebral I/R model. However, they promote antioxidative stress, anti-apoptotic benefits, and protective effects in the rat cardiac damage model (Han et al., 2009; Harima et al., 2015; Lin et al., 2020). To evaluate whether PAGly acts by inhibiting the  $\beta$ 2AR, fenoterol was employed (Maciag et al., 2023). Fenoterol reverses the protective effect of microglia-conditioned medium on neurons after PAGly intervention and aggravates nerve injury, thereby increasing neuronal apoptosis that was already reduced. Overall, the data validated that PAGly attenuates microglial inflammation and exerts neuroprotection by inhibiting  $\beta$ 2AR (Fig. 5). However, when  $\beta$ 2AR is reactivated, this protective effect is lost,

implying that PAGly can only suppress  $\beta$ 2AR, which is an active inhibitor, rather than regulate its expression level.

Crossing the BBB is a significant challenge for pharmacotherapies for potent central nervous system effects. PAGly is a small molecule that can freely cross the BBB and exert therapeutic effects within the brain's parenchyma. Furthermore, it can attenuate microglial-mediated inflammatory responses and diminish neuronal apoptosis, which distinguishes it from ready-availability therapeutic drugs in its efficacy and cost-effectiveness. These attributes render PAGly a compelling candidate for early-stage intervention in cerebral I/R injuries, highlighting its potential to address a critical need within CNS pharmacotherapy.

There are certain limitations of this study. First, our study focused exclusively on the role of PAGly during the acute phase of cerebral I/R injury, and its long-term effects remain insufficiently explored. Second, the pharmacokinetics of PAGly following administration, as well as the precise mechanisms by which it modulates  $\beta$ 2AR, have not been thoroughly investigated. Future research with expanded sample sizes will aim to address these gaps and further assess the therapeutic potential of PAGly.

#### CRediT authorship contribution statement

**Wenjie Hu:** Writing – original draft, Methodology, Funding acquisition, Conceptualization. **Xueyan Kuang:** Methodology, Investigation. **Yao Zhang:** Investigation. **Yimin Luo:** Writing – original draft, Methodology. **Litao Zhang:** Writing – review & editing, Supervision, Conceptualization.

#### Funding

This work was supported by the Medical and Health Science and Technology Development Project of Shandong Province (202102060559) and the Research Fund for Academician LinHe New Medicine (JYHL2022MS16).

#### Animal Ethics

Experimental procedures on all animals were performed in accordance with the guidelines of the Animal Care Committee of Jining Medical University and endorsed by the Animal Care Committee of Jining Medical University on January 02, 2023 (No. JNMC-2023-DW-085).

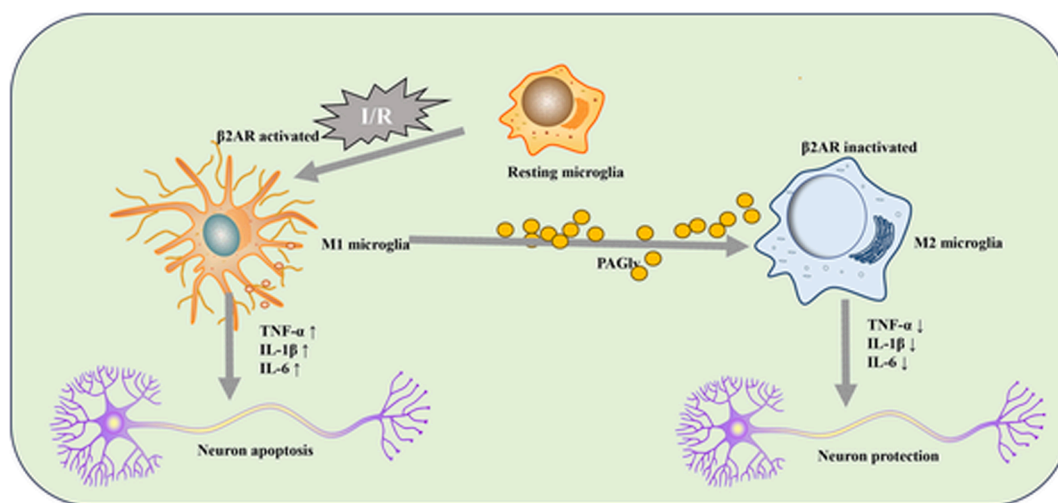


**Fig. 5.** The mechanism for the neuroprotective effects of PAGly via  $\beta$ 2AR Following cerebral I/R injury, microglia across different brain regions become activated, showing heightened activation of  $\beta$ 2AR, resulting in enlarged cell bodies and increased secretion of IL-1 $\beta$ , IL-6 and TNF- $\alpha$ . Upon interacting with  $\beta$ 2AR on microglia, PAGly effectively suppresses the production of inflammatory cytokines, consequently safeguarding neurons.



## Declaration of competing interest

The authors declare that they have no known competing financial interests or personal relationships that could have appeared to influence the work reported in this paper.

## References

- Adeyemi, J.A., Peters, S.O., De Donato, M., Cervantes, A.P., Ogunade, I.M., 2020. Effects of a blend of *Saccharomyces cerevisiae*-based direct-fed microbial and fermentation products on plasma carbonyl-metabolome and fecal bacterial community of beef steers. *J. Anim. Sci. Biotechnol.* 11, 14. <https://doi.org/10.1186/s40104-019-0419-5>.
- Benakis, C., Brea, D., Caballero, S., Faraco, G., Moore, J., Murphy, M., Sita, G., Racchumi, G., Ling, L., Pamer, E.G., Iadecola, C., Anrather, J., 2016. Commensal microbiota affects ischemic stroke outcome by regulating intestinal  $\gamma\delta$  T cells. *Nat. Med.* 5, 516–523. <https://doi.org/10.1038/nm.4068>.
- Chen, B., Kong, X., Li, Z., Hu, W., Zhou, H., Gao, J., Cui, Y., Li, S., Wan, Q., Feng, Y., 2022. Downregulation of NF- $\kappa$ B by Shp-1 alleviates cerebral venous sinus thrombosis-induced brain edema via suppression of AQP4. *J. Stroke Cerebrovasc. Dis.* 31, 106570. <https://doi.org/10.1016/j.jstrokecerebrovasdis.2022.106570>.
- Damo, E., Agarwal, A., Simonetti, M., 2023. Activation of  $\beta$ 2-adrenergic receptors in microglia alleviates neuropathic hypersensitivity in mice. *Cells*. 12. <https://doi.org/10.3390/cells12020284>.
- Ermine, C.M., Bivard, A., Parsons, M.W., Baron, J.C., 2021. The ischemic penumbra: from concept to reality. *Int. J. Stroke*. 16, 497–509. <https://doi.org/10.1177/1747493020975229>.
- Fan, J., Li, X., Yu, X., Liu, Z., Jiang, Y., Fang, Y., Zong, M., Suo, C., Man, Q., Xiong, L., 2023. Global burden, risk factor analysis, and prediction study of ischemic stroke, 1990–2030. *Neurology*. 101, e137–e150. <https://doi.org/10.1212/wnl.0000000000207387>.
- Gargiulo, S., Greco, A., Gramanzini, M., Esposito, S., Affuso, A., Brunetti, A., Vesce, G., 2012. Mice anesthesia, analgesia, and care, Part I: anesthetic considerations in preclinical research. *ILAR J.* 53, e55–e69. <https://doi.org/10.1093/ilar.53.1.55>.
- Hacke, W., Donnan, G., Fieschi, C., Kaste, M., von Kummer, R., Broderick, J.P., Brodt, T., Frankel, M., Grotta, J.C., Haley Jr., E.C., Kwiatkowski, T., Levine, S.R., Lewandowski, C., Lu, M., Lyden, P., Marler, J.R., Patel, S., Tilley, B.C., Albers, G., Bluhmki, E., Wilhelm, M., Hamilton, S., 2004. Association of outcome with early stroke treatment: pooled analysis of ATLANTIS, ECASS, and NINDS rt-PA stroke trials. *Lancet*. 363, 768–774. [https://doi.org/10.1016/S0140-6736\(04\)15692-4](https://doi.org/10.1016/S0140-6736(04)15692-4).
- Han, R.Q., Ouyang, Y.B., Xu, L., Agrawal, R., Patterson, A.J., Giffard, R.G., 2009. Postischemic brain injury is attenuated in mice lacking the beta2-adrenergic receptor. *Anesth. Analg.* 108, 280–287. <https://doi.org/10.1213/ane.0b013e318187ba6b>.
- Harima, M., Arumugam, S., Wen, J., Pitchaimani, V., Karuppagounder, V., Afrin, M.R., Sreedhar, R., Miyashita, S., Nomoto, M., Ueno, K., Nakamura, M., Watanabe, K., 2015. Effect of carvedilol against myocardial injury due to ischemia-reperfusion of the brain in rats. *Exp. Mol. Pathol.* 98, 558–562. <https://doi.org/10.1016/j.yexmp.2015.04.001>.
- Hu, W., Kong, X., Wang, H., Li, Y., Luo, Y., 2022. Ischemic stroke and intestinal flora: an insight into brain-gut axis. *Eur. J. Med. Res.* 1, 73. <https://doi.org/10.1186/s40001-022-00691-2>.
- Jin, R., Liu, L., Zhang, S., Nanda, A., Li, G., 2013. Role of inflammation and its mediators in acute ischemic stroke. *J. Cardiovasc. Transl. Res.* 6, 834–851. <https://doi.org/10.1007/s12265-013-9508-6>.
- Jin, L., Zhu, Z., Hong, L., Qian, Z., Wang, F., Mao, Z., 2023. ROS-responsive 18 $\beta$ -glycyrrhetic acid-conjugated polymeric nanoparticles mediate neuroprotection in ischemic stroke through HMGB1 inhibition and microglia polarization regulation. *Bioact. Mater.* 19, 38–49. <https://doi.org/10.1016/j.bioactmat.2022.03.040>.
- Kristiansen, R.G., Rose, C.F., Fuskevåg, O.M., Mæhre, H., Revhaug, A., Jalan, R., Ytrebø, L.M., 2014. L-Ornithine phenylacetate reduces ammonia in pigs with acute liver failure through phenylacetylglutamine formation: a novel ammonia-lowering pathway. *Am. J. Physiol. Gastrointest. Liver Physiol.* 307 (10). <https://doi.org/10.1152/ajpgi.00244.2014>.
- Liang, Z., Lou, Y., Hao, Y., Li, H., Feng, J., Liu, S., 2023. The relationship of astrocytes and microglia with different stages of ischemic stroke. *Curr. Neuropharmacol.* 21, 2465–2480. <https://doi.org/10.2174/1570159x21666230718104634>.
- Liao, S., Wu, J., Liu, R., Wang, S., Luo, J., Yang, Y., Qin, Y., Li, T., Zheng, X., Song, J., Zhao, X., Xiao, C., Zhang, Y., Bian, L., Jia, P., Bai, Y., Zheng, X., 2020. A novel compound DBZ ameliorates neuroinflammation in LPS-stimulated microglia and ischemic stroke rats: role of Akt(Ser473)/GSK3 $\beta$ (Ser9)-mediated Nrf2 activation. *Redox Biol.* 36, 101644. <https://doi.org/10.1016/j.redox.2020.101644>.
- Lin, J., Fan, L., Han, Y., Guo, J., Hao, Z., Cao, L., Kang, J., Wang, X., He, J., Li, J., 2021. The mTORC1/eIF4E/HIF-1 $\alpha$  pathway mediates glycolysis to support brain hypoxia resistance in the gansu zokor. *Eospalax Cansus. Front Physiol.* 12, 626240. <https://doi.org/10.3389/fphys.2021.626240>.
- Lin, S.Y., Wang, Y.Y., Chang, C.Y., Wu, C.C., Chen, W.Y., Kuan, Y.H., Liao, S.L., Chen, C. J., 2020. Effects of  $\beta$ -adrenergic blockade on metabolic and inflammatory responses in a rat model of ischemic stroke. *Cells*. 9, 1373. <https://doi.org/10.3390/cells9061373>.
- Liu, B., Li, L., Zhang, Q., Chang, N., Wang, D., Shan, Y., Li, L., Wang, H., Feng, H., Zhang, L., Brann, D.W., Wan, Q., 2010. Preservation of GABAA receptor function by PTEN inhibition protects against neuronal death in ischemic stroke. *Stroke* 41, 1018–1026. <https://doi.org/10.1161/strokeaha.110.579011>.
- Liu, M., Xu, Z., Wang, L., Zhang, L., Liu, Y., Cao, J., Fu, Q., Liu, Y., Li, H., Lou, J., Hou, W., Mi, W., Ma, Y., 2020. Cottonseed oil alleviates ischemic stroke injury by inhibiting the inflammatory activation of microglia and astrocyte. *J. Neuroinflammation* 17, 270. <https://doi.org/10.1186/s12974-020-01946-7>.
- Longa, E.Z., Weinstein, P.R., Carlson, S., Cummins, R., 1989. Reversible middle cerebral artery occlusion without craniectomy in rats. *Stroke* 20, 84–91. <https://doi.org/10.1161/01.str.20.1.84>.
- Maciag, M., Plazinski, W., Pulawski, W., Kolinski, M., Jozwiak, K., Plazinska, A., 2023. A comprehensive pharmacological analysis of fenoterol and its derivatives to unravel the role of  $\beta$ (2)-adrenergic receptor in zebrafish. *Biomed. Pharmacother.* 160, 114355. <https://doi.org/10.1016/j.biopha.2023.114355>.
- Merenthaler, I., Dellovade, T.L., Shughrue, P.J., 2003. Neuroprotection by estrogen in animal models of global and focal ischemia. *Ann. N. Y. Acad. Sci.* 1007, 89–100. <https://doi.org/10.1196/annals.1286.009>.
- Nair, K.G.S., Ramaiyan, V., Sukumaran, S.K., 2018. Enhancement of drug permeability across blood brain barrier using nanoparticles in meningitis. *Inflammopharmacology* 26, 675–684. <https://doi.org/10.1007/s10787-018-0468-y>.
- Nemet, I., Saha, P.P., Gupta, N., Zhu, W., Romano, K.A., Skye, S.M., Cajka, T., Mohan, M. L., Li, L., Wu, Y., Funabashi, M., Ramer-Tait, A.E., Naga Prasad, S.V., Fiehn, O., Rey, F.E., Tang, W.H.W., Fischbach, M.A., DiDonato, J.A., Hazen, S.L., 2020. A cardiovascular disease-linked gut microbial metabolite acts via adrenergic receptors. *Cell* 180, 862–877.e822. <https://doi.org/10.1016/j.cell.2020.02.016>.
- Onasanwo, S.A., Velagapudi, R., El-Bakoush, A., Olajide, O.A., 2016. Inhibition of neuroinflammation in BV2 microglia by the biflavonoid kolaviron is dependent on the Nrf2/ARE antioxidant protective mechanism. *Mol. Cell Biochem.* 414, 23–36. <https://doi.org/10.1007/s11010-016-2655-8>.
- Peng, L., Hu, G., Yao, Q., Wu, J., He, Z., Law, B.Y., Hu, G., Zhou, X., Du, J., Wu, A., Yu, L., 2022. Microglia autophagy in ischemic stroke: a double-edged sword. *Front. Immunol.* 13, 1013311. <https://doi.org/10.3389/fimmu.2022.1013311>.
- Prabhakaran, S., Ruff, I., Bernstein, R.A., 2015. Acute stroke intervention: a systematic review. *J. Am. Med. Assoc.* 313, 1451–1462. <https://doi.org/10.1001/jama.2015.3058>.
- Romano, K.A., Nemet, I., Prasad Saha, P., Haghighi, A., Li, X.S., Mohan, M.L., Lovano, B., Castel, L., Witkowski, M., Buffa, J.A., Sun, Y., Li, L., Menge, C.M., Demuth, I., König, M., Steinhagen-Thiessen, E., DiDonato, J.A., Deb, A., Bäckhed, F., Tang, W.H. W., Naga Prasad, S.V., Landmesser, U., Van Wagoner, D.R., Hazen, S.L., 2023. Gut microbiota-generated phenylacetylglutamine and heart failure. *Circ. Heart Fail.* 16, e009972. <https://doi.org/10.1161/circheartfailure.122.009972>.
- Sugama, S., Takenouchi, T., Hashimoto, M., Ohata, H., Takenaka, Y., Kakinuma, Y., 2019. Stress-induced microglial activation occurs through  $\beta$ -adrenergic receptor: noradrenaline as a key neurotransmitter in microglial activation. *J. Neuroinflammation* 16 (266), 10.
- Tanaka, K.F., Kashima, H., Suzuki, H., Ono, K., Sawada, M., 2002. Existence of functional beta-1 and beta-2-adrenergic receptors on microglia. *J. Neurosci. Res.* 70, 232–237. <https://doi.org/10.1002/jnr.10399>.
- Wang, W., Chen, J., Li, X.G., Xu, J., 2016. Anti-inflammatory activities of fenoterol through  $\beta$ -arrestin-2 and inhibition of AMPK and NF- $\kappa$ B activation in AICAR-induced THP-1 cells. *Biomed. Pharmacother.* 84, 185–190. <https://doi.org/10.1016/j.biopha.2016.09.044>.
- Wang, D., Liu, F., Zhu, L., Lin, P., Han, F., Wang, X., Tan, X., Lin, L., Xiong, Y., 2020. FGF21 alleviates neuroinflammation following ischemic stroke by modulating the temporal and spatial dynamics of microglia/macrophages. *J. Neuroinflammation* 17, 257. <https://doi.org/10.1186/s12974-020-01921-2>.
- Wang, H., Ma, W., Hu, W., Li, X., Shen, N., Li, Z., Kong, X., Lin, T., Gao, J., Zhu, T., Che, F., Chen, J., Wan, Q., 2024. Cathodal bilateral transcranial direct-current stimulation regulates selenium to confer neuroprotection after rat cerebral ischaemia-reperfusion injury. *J. Physiol.* 602, 1175–1197. <https://doi.org/10.1113/jp285806>.
- Wang, S., Shi, X., Xiong, T., Chen, Q., Yang, Y., Chen, W., Zhang, K., Nan, Y., Huang, Q., Ai, K., 2024. Inhibiting mitochondrial damage for efficient treatment of cerebral ischemia-reperfusion injury through sequential targeting nanomedicine of neuronal mitochondria in affected brain tissue. *Adv. Mater.*, e2409529 <https://doi.org/10.1002/adma.202409529>.
- Wu, T., Tong, M., Chu, A., Wu, K., Niu, X., Zhang, Z., 2022. PM2.5-induced programmed myocardial cell death via mPTP opening results in deteriorated cardiac function in HFpEF mice. *Cardiovasc. Toxicol.* 22, 746–762. <https://doi.org/10.1007/s12012-022-09753-7>.
- Wu, L., Xiong, X., Wu, X., Ye, Y., Jian, Z., Zhi, Z., Gu, L., 2020. Targeting oxidative stress and inflammation to prevent ischemia-reperfusion injury. *Front. Mol. Neurosci.* 13, 28. <https://doi.org/10.3389/fnmol.2020.00028>.
- Xu, X., Cui, Y., Li, C., Wang, Y., Cheng, J., Chen, S., Sun, J., Ren, J., Yao, X., Gao, J., Huang, X., Wan, Q., Wang, Q., 2021. SETD3 downregulation mediates PTEN upregulation-induced ischemic neuronal death through suppression of actin polymerization and mitochondrial function. *Mol. Neurobiol.* 58, 4906–4920. <https://doi.org/10.1007/s12035-021-02459-x>.
- Xu, X., Lu, W.J., Shi, J.Y., Su, Y.L., Liu, Y.C., Wang, L., Xiao, C.X., Chen, C., Lu, Q., 2021. The gut microbial metabolite phenylacetylglutamine protects against cardiac injury caused by ischemia/reperfusion through activating  $\beta$ 2AR. *Arch. Biochem. Biophys.* 697, 108720. <https://doi.org/10.1016/j.abb.2020.108720>.
- Xu, J., Zhang, L., Li, M., He, X., Luo, J., Wu, R., Hong, Z., Zheng, H., Hu, X., 2023. TREM2 mediates physical exercise-promoted neural functional recovery in rats with ischemic stroke via microglia-promoted white matter repair. *J. Neuroinflammation* 20, 50. <https://doi.org/10.1186/s12974-023-02741-w>.
- Yang, S.X., Polley, E., Lipkowitz, S., 2016. New insights on PI3K/AKT pathway alterations and clinical outcomes in breast cancer. *Cancer Treat. Rev.* 45, 87–96. <https://doi.org/10.1016/j.ctrv.2016.03.004>.

Zhang, Z., Wang, Q., Zhao, X., Shao, L., Liu, G., Zheng, X., Xie, L., Zhang, Y., Sun, C., Xu, R., 2020. YTHDC1 mitigates ischemic stroke by promoting Akt phosphorylation through destabilizing PTEN mRNA. *Cell Death Dis.* 11, 977. <https://doi.org/10.1038/s41419-020-03186-2>.

Zhou, T., Liu, Y., Yang, Z., Ni, B., Zhu, X., Huang, Z., Xu, H., Feng, Q., Lin, X., He, C., Liu, X., 2021. IL-17 signaling induces iNOS<sup>+</sup> microglia activation in retinal vascular diseases. *Glia.* 69, 2644–2657. <https://doi.org/10.1002/glia.24063>.

Zhu, H., Jian, Z., Zhong, Y., Ye, Y., Zhang, Y., Hu, X., Pu, B., Gu, L., Xiong, X., 2021. Janus kinase inhibition ameliorates ischemic stroke injury and neuroinflammation through reducing NLRP3 inflammasome activation via JAK2/STAT3 pathway inhibition. *Front. Immunol.* 12, 714943. <https://doi.org/10.3389/fimmu.2021.714943>.